

Numerical Studies of Gas-Liquid-Fueled Two-Phase Detonation by Using Improved CE/SE method

D. L. Zhang

State Key Laboratory of High Temperature Gas Dynamics, Institute of Mechanics, CAS,

15 Beisihuanxi Road, Haidian District, Beijing 100190, China

**Corresponding author. Email: DLZhang@imech.ac.cn*

Abstract: The gas-liquid-fueled two-phase detonation has very complex phenomena and characters. Until now they are studied mainly by experiments, because complex interactions between the two phases and chemical reactions models make numerical simulations very difficult. In the paper, numerical simulations of gas-liquid-fueled two-phase detonation have been performed by using an improved Space-Time Conservation Element and Solution Element (CE/SE) method. The Eulerian Two-Fluid Model and Eulerian-Lagrangian Particle-Trace Model were adopted already. Numerical results were compared with some experiments and characters of gas-liquid-fueled two-phase detonation were analyzed. All of them show that the complex phenomena of gas-liquid-fueled two-phase detonation can be simulated. The improved CE/SE scheme has the features of high resolution, simple form and robustness.

Keywords: gas-liquid-fueled two-phase flow; detonation; chemical reactions; CE/SE method;

1 Introduction

The formation and propagation of detonation is a very complicated phenomenon [1] [2]. For a long time the detonation phenomena are studied mainly by experiments. However, in the last 25 years the numerical simulations have improved immensely as a result of major progress in both computational methods and available computer. Especially in last recent decades of development, the mechanism recognition of detonations in gaseous fuel-oxidizer mixtures has made large progresses and its numerical simulation can be basically achieved [3]. But our understanding of the initiation, formation, structure and stability of detonations in gas-liquid-fueled two-phase mixtures are still more primitive than for detonations in gaseous fuel-oxidizer mixtures [4].

The lack of knowledge of the features of gas-liquid-fueled detonations can be partly ascribed to the fact that the governing parameters of gas-liquid-fueled mixtures are far more than that of gaseous mixtures. Indeed, apart from the chemical composition and initial pressure and temperature of the mixture, one should take into account atomization, droplet breakup and vaporization, droplet size and shape as well as droplet distribution, etc. The latter effects may play a major role in gas-liquid-fueled two-phase detonations [5]. They will induce that the detonation processes are very complex and detonation zone thickness is at least a few times larger than that in gaseous fuel-oxidizer mixtures. All these features result in mathematical and physical difficulties.

The difficulties of numerical simulation of gas-liquid-fueled detonation are mainly due to its complex physical and chemical phenomena as well as determination for governing parameters of gas-liquid-fueled mixtures. In the simulations of gas-liquid-fueled detonation there are two primary factors: One is the strong discontinuity surface in detonation waves; another is the process of energy release in the flow field. These factors depend on numerical schemes and chemical reaction models respectively [6] [7].

In this paper an efficient and accurate Eulerian-Lagrangian Particle-Trace Model for

gas-liquid-fueled two-phase detonations was constructed and compared with the normal Eulerian Two-Fluid Model. A new two-dimensional CE/SE scheme with two-order accuracy with a hexahedral mesh was deduced. The simplified chemical reaction models were adopted. The gas-liquid-fueled two-phase detonation in liquid-fueled C_6H_{14} -air system and liquid-fueled $C_{10}H_{22}$ - O_2 /air systems were simulated. The numerical results were discussed and compared with corresponding results by C-J theory and experiments. All of these show that Eulerian Two-Fluid Model, Eulerian-Lagrangian Particle-Trace Model and the improved CE/SE schemes with two-order accuracy are reasonable and feasible. The main features and characters of complex gas-liquid-fueled two-phase detonation can be successfully simulated.

2 Governing Equations and Chemical Reaction Model

2.1 Governing Equations

In this paper, an Eulerian-Lagrangian Particle-Trace Model is introduced for treating the gas-liquid-fueled two-phase detonations. The droplet phase is considered as continuous and homogeneous medium and all droplets can be traced by Lagrangian method.

Following assumptions are made about present model: the gas phase behaves as an ideal gas; the temperature of all gaseous species is the same; there are no process of collision, coalescence and fragmentation in droplet phase; the shape of droplets always keeps to be spherical; the temperature distribution in droplet phase is uniform; the volume occupied by droplets is negligible when it compares with the volume of gas; chemical reactions occur only in the gas phase; if chemical reaction occurs, the chemical energy is absorbed only by gas.

Under the above assumptions, the gas-phase is governed by Eulerian equations:

$$\frac{\partial \mathbf{Q}}{\partial t} + \frac{\partial \mathbf{E}}{\partial x} + \frac{\partial \mathbf{F}}{\partial y} = \mathbf{S}. \quad (1)$$

In Eq. (1), \mathbf{Q} is the vector of conserved variables, \mathbf{E} and \mathbf{F} are the conservation flux vectors in x- and y-directions, \mathbf{S} is the source term vector. Combined with chemical reaction and phase transition, the expressions of \mathbf{Q} , \mathbf{E} , \mathbf{F} , \mathbf{S} are as follows

$$\mathbf{Q} = \begin{pmatrix} \rho_i \\ \rho u \\ \rho v \\ e \end{pmatrix}, \quad \mathbf{E} = \begin{pmatrix} \rho_i u \\ \rho u^2 + p \\ \rho uv \\ (e + p)u \end{pmatrix}, \quad \mathbf{F} = \begin{pmatrix} \rho_i v \\ \rho uv \\ \rho v^2 + p \\ (e + p)v \end{pmatrix}$$

$$\text{and } \mathbf{S} = \begin{pmatrix} \omega_i + \delta \sum_1^{N_p} \frac{I_{pk}}{dV_k} \\ \sum_1^{N_p} \frac{-f_{xk} + u_{pk} I_{pk}}{dV_k} \\ \sum_1^{N_p} \frac{-f_{yk} + v_{pk} I_{pk}}{dV_k} \\ \sum_1^{N_p} \frac{-q_{dk} - (u_{pk} f_{xk} + v_{pk} f_{yk}) + \left(e_{pk} + \frac{u_{pk}^2 + v_{pk}^2}{2} \right) I_{pk}}{dV_k} \end{pmatrix}. \quad (2)$$

The Lagrangian governing equations for the k -th droplet are as follows:

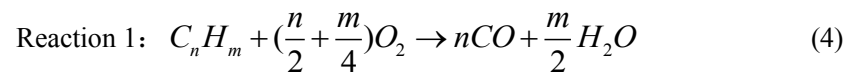
$$\left\{ \begin{array}{l} \frac{dm_{pk}}{dt} = -I_{pk} \\ \frac{dx_{pk}}{dt} = u_{pk} \\ \frac{dy_{pk}}{dt} = v_{pk} \\ m_{pk} \frac{du_{pk}}{dt} = f_{xk} \\ m_{pk} \frac{dv_{pk}}{dt} = f_{yk} \\ C_v \frac{dT_{pk}}{dt} = q_{dk} \end{array} \right. \quad (3)$$

Here ρ_i (i from 1 to Ns) is the mass density of the i -th species (especially, ρ_1 is defined as the density of fuel gas), Ns is the number of considered species, ω_i is the production rate of the i -th species. ρ , u , v , p and e are the total density, the velocity components of x -direction and y -direction, the pressure, and the total energy per unit volume of gas phase, respectively. Accordingly, m_{pk} , x_{pk} , y_{pk} , u_{pk} , v_{pk} , T_{pk} , e_{pk} and I_{pk} denote the mass, the position coordinates components and the velocity components, temperature, the internal energy per unit mass and atomization rate of the k -th (k from 1 to Np) droplet, respectively. Np is the number of initial droplets, which is determined by the equivalence ratio of gas-liquid-fueled mixture. f_{xk} and f_{yk} are the force components acting on the k -th droplet. q_{dk} is the convection heat transfer between gas mixtures and the k -th droplet. C_v is the capacity of liquid fuel. dV_k is the volume of gas phase influenced by the k -th droplet, which is related to the Euler grid. When $i=1$, $\delta=1$, otherwise, $\delta=0$.

The dynamic interaction of droplets with the gaseous flow could bring to instability of the interface and atomization of droplets. According to boundary layer theory, the atomization rate of droplets and the force components acting on the k -th droplet as well as convection heat transfer between gas mixtures and the k -th droplet were derived by references [8] [9].

2.2 Chemical Reaction Models

CO , CO_2 and H_2O are the main product of the chemical reaction between hydrocarbon and oxygen. In present study, to avoid complicate the problem and save computing resources, the following three main global reaction involving five species are considered:



The expression of each chemical reaction rate RP_k is available in Ref. [10-11]. Then, production rate of each chemical species ω_i is expressed as:

$$\omega_i = W_i \sum_{k=1}^{Nr} (v_{ki}'' - v_{ki}') RP_k, \quad (7)$$

where W_i is the molecular weight of the i -th species, Nr is the number of chemical reactions, v_{ki}'

and v_{ki}'' are the stoichiometric coefficients of the i -th species in the k -th chemical reaction.

3 Improved CE/SE Scheme

The CE/SE method was originally proposed by Chang and co-workers [12-13], which is a completely new numerical framework for solving hyperbolic conservation equations. According to principle of Chang designed two grid types, we design more general structures of two-dimensional CEs and SEs (Fig.1) [14]. New two-dimensional CE/SE schemes can be constructed sententiously and three-dimensional scheme can be extend easily.

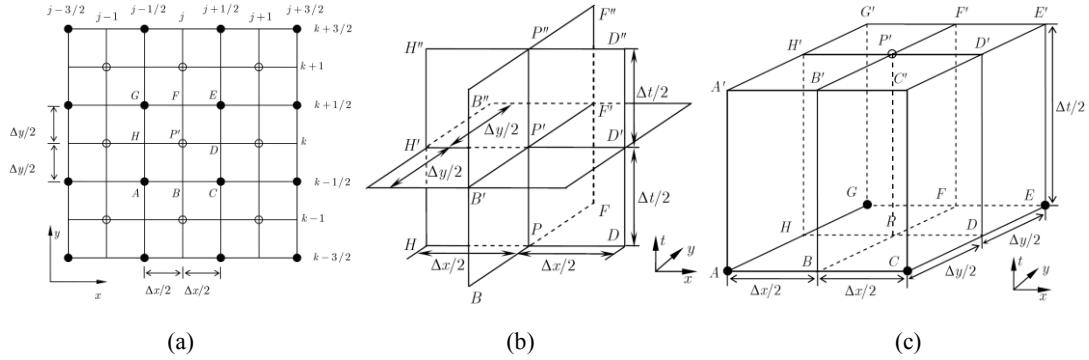


Fig.1 (a) Mesh points projection on xy plane (b)SE (c)CEs (in this work)

3.1 Improved CE/SE Scheme with the second order accuracy

Consider the two-dimensional conservation equations:

$$\frac{\partial \mathbf{Q}}{\partial t} + \frac{\partial \mathbf{E}}{\partial x} + \frac{\partial \mathbf{F}}{\partial y} = 0, \quad (8)$$

Then because Eq. (8) can be expressed as $\nabla \cdot \mathbf{H} = 0$ with $\mathbf{H} = (\mathbf{Q}, \mathbf{E}, \mathbf{F})$. The Gauss' divergence theorem in the space-time E_3 implies that Eq. (8) is the differential form of the integral conservation law:

$$\int_{S(V)} \hat{\mathbf{n}} \cdot \mathbf{H} \, d\sigma = 0 \quad (9)$$

where $S(V)$ is the boundary of an arbitrary space-time region V in E_3 ; $d\mathbf{s} = d\sigma \cdot \mathbf{n}$ with $d\sigma$ and \mathbf{n} , respectively, being the area and the unit outward normal vector of a surface element on $S(V)$.

For an arbitrary grid point P' , we define a solution element SE (P') that constituted by the three vertical planes intersecting at P' as demonstrating in Fig. 1 (b). Assuming that \mathbf{E} , \mathbf{F} and \mathbf{Q} at point (x, y, t) in SE (P') are approximated by the second-order Taylor's expansions at $P'(j, k, n)$:

$$\begin{aligned} \mathbf{Q}(\delta x, \delta y, \delta t)_{P'} &= (\mathbf{Q})_{P'} + (\mathbf{Q}_x)_{P'} \delta x + (\mathbf{Q}_y)_{P'} \delta y + (\mathbf{Q}_t)_{P'} \delta t \\ &\quad + \frac{1}{2} (\mathbf{Q}_{xx})_{P'} (\delta x)^2 + \frac{1}{2} (\mathbf{Q}_{yy})_{P'} (\delta y)^2 + \frac{1}{2} (\mathbf{Q}_{tt})_{P'} (\delta t)^2, \\ &\quad + (\mathbf{Q}_{xy})_{P'} \delta x \delta y + (\mathbf{Q}_{xt})_{P'} \delta x \delta t + (\mathbf{Q}_{yt})_{P'} \delta y \delta t \end{aligned} \quad (10)$$

$$\begin{aligned} \mathbf{E}(\delta x, \delta y, \delta t)_{P'} &= (\mathbf{E})_{P'} + (\mathbf{E}_x)_{P'} \delta x + (\mathbf{E}_y)_{P'} \delta y + (\mathbf{E}_t)_{P'} \delta t \\ &\quad + \frac{1}{2} (\mathbf{E}_{xx})_{P'} (\delta x)^2 + \frac{1}{2} (\mathbf{E}_{yy})_{P'} (\delta y)^2 + \frac{1}{2} (\mathbf{E}_{tt})_{P'} (\delta t)^2, \\ &\quad + (\mathbf{E}_{xy})_{P'} \delta x \delta y + (\mathbf{E}_{xt})_{P'} \delta x \delta t + (\mathbf{E}_{yt})_{P'} \delta y \delta t \end{aligned} \quad (11)$$

$$\begin{aligned} \mathbf{F}(\delta x, \delta y, \delta t)_{P'} &= (\mathbf{F})_{P'} + (\mathbf{F}_x)_{P'} \delta x + (\mathbf{F}_y)_{P'} \delta y + (\mathbf{F}_t)_{P'} \delta t \\ &\quad + \frac{1}{2} (\mathbf{F}_{xx})_{P'} (\delta x)^2 + \frac{1}{2} (\mathbf{F}_{yy})_{P'} (\delta y)^2 + \frac{1}{2} (\mathbf{F}_{tt})_{P'} (\delta t)^2, \\ &\quad + (\mathbf{F}_{xy})_{P'} \delta x \delta y + (\mathbf{F}_{xt})_{P'} \delta x \delta t + (\mathbf{F}_{yt})_{P'} \delta y \delta t \end{aligned} \quad (12)$$

Where $\delta x=x-x_{P'}$, $\delta y=y-y_{P'}$, $\delta t=t-t_{P'}$, $x_{P'}$, $y_{P'}$ and $t_{P'}$ are the position coordinates of point P' , but $(V)_{P'}$, $(V_x)_{P'}$, $(V_y)_{P'}$, $(V_t)_{P'}$, $(V_{xx})_{P'}$, $(V_{yy})_{P'}$, $(V_{tt})_{P'}$, $(V_{xy})_{P'}$, $(V_{xt})_{P'}$ and $(V_{yt})_{P'}$ are the constant values of V , its first-order and second-order derivative on x , y and t directions at point P' , respectively, in which V denotes \mathbf{Q} , \mathbf{E} and \mathbf{F} . Substituting Eq. (10), (11) and (12) into Eq. (8), it can obtain:

$$\begin{cases} (\mathbf{Q}_t)_{P'} = -(\mathbf{E}_x)_{P'} - (\mathbf{F}_y)_{P'} \\ (\mathbf{Q}_{xt})_{P'} = -(\mathbf{E}_{xx})_{P'} - (\mathbf{F}_{xy})_{P'} \\ (\mathbf{Q}_{yt})_{P'} = -(\mathbf{E}_{xy})_{P'} - (\mathbf{F}_{yy})_{P'} \\ (\mathbf{Q}_{tt})_{P'} = -(\mathbf{E}_{xt})_{P'} - (\mathbf{F}_{yt})_{P'} \end{cases} \quad (13)$$

The above equations imply that the variables required in computation are $(\mathbf{Q})_{P'}$ and its first and second order space derivatives $(\mathbf{Q}_x)_{P'}$, $(\mathbf{Q}_y)_{P'}$, $(\mathbf{Q}_{xx})_{P'}$, $(\mathbf{Q}_{yy})_{P'}$ and $(\mathbf{Q}_{xy})_{P'}$.

Assuming flux vectors in every CE satisfy the integral conservation law, and the integrating Eq. (9) on the surfaces of CE (P') with the aid of Eq. (10), (11) and (12), we can obtained:

$$(\mathbf{Q})_{P'} + \frac{\Delta x^2}{24} (\mathbf{Q}_{xx})_{P'} + \frac{\Delta y^2}{24} (\mathbf{Q}_{yy})_{P'} = \frac{1}{4} \left(\bar{\mathbf{Q}} + \frac{\Delta t}{\Delta x} \bar{\mathbf{E}} + \frac{\Delta t}{\Delta y} \bar{\mathbf{F}} \right) \quad (14)$$

Define the following functions as:

$$\begin{aligned} \hat{\mathbf{Q}}(\delta x, \delta y, \delta t)_{P'} &= (\mathbf{Q})_{P'} + (\mathbf{Q}_x)_{P'} \delta x + (\mathbf{Q}_y)_{P'} \delta y + (\mathbf{Q}_t)_{P'} \delta t \\ &\quad + \frac{1}{6} (\mathbf{Q}_{xx})_{P'} (\delta x)^2 + \frac{1}{6} (\mathbf{Q}_{yy})_{P'} (\delta y)^2 + (\mathbf{Q}_{xy})_{P'} \delta x \delta y \\ \hat{\mathbf{E}}(\delta x, \delta y, \delta t)_{P'} &= (\mathbf{E})_{P'} + (\mathbf{E}_x)_{P'} \delta x + (\mathbf{E}_y)_{P'} \delta y + (\mathbf{E}_t)_{P'} \delta t \\ &\quad + \frac{1}{6} (\mathbf{E}_{yy})_{P'} (\delta y)^2 + \frac{1}{6} (\mathbf{E}_{tt})_{P'} (\delta t)^2 + (\mathbf{E}_{yt})_{P'} \delta y \delta t \\ \hat{\mathbf{F}}(\delta x, \delta y, \delta t)_{P'} &= (\mathbf{F})_{P'} + (\mathbf{F}_x)_{P'} \delta x + (\mathbf{F}_y)_{P'} \delta y + (\mathbf{F}_t)_{P'} \delta t \\ &\quad + \frac{1}{6} (\mathbf{F}_{xx})_{P'} (\delta x)^2 + \frac{1}{6} (\mathbf{F}_{tt})_{P'} (\delta t)^2 + (\mathbf{F}_{xt})_{P'} \delta x \delta t \end{aligned} \quad (15)$$

So the $\bar{\mathbf{Q}}$, $\bar{\mathbf{E}}$ and $\bar{\mathbf{F}}$ in Eq. (14) can be expressed as:

$$\begin{aligned} \bar{\mathbf{Q}} &= \hat{\mathbf{Q}}\left(\frac{\Delta x}{4}, \frac{\Delta y}{4}, 0\right)_A + \hat{\mathbf{Q}}\left(-\frac{\Delta x}{4}, \frac{\Delta y}{4}, 0\right)_C + \hat{\mathbf{Q}}\left(-\frac{\Delta x}{4}, -\frac{\Delta y}{4}, 0\right)_E + \hat{\mathbf{Q}}\left(\frac{\Delta x}{4}, -\frac{\Delta y}{4}, 0\right)_G \\ \bar{\mathbf{E}} &= \hat{\mathbf{E}}\left(0, \frac{\Delta y}{4}, \frac{\Delta t}{4}\right)_A - \hat{\mathbf{E}}\left(0, \frac{\Delta y}{4}, \frac{\Delta t}{4}\right)_C - \hat{\mathbf{E}}\left(0, -\frac{\Delta y}{4}, \frac{\Delta t}{4}\right)_E + \hat{\mathbf{E}}\left(0, -\frac{\Delta y}{4}, \frac{\Delta t}{4}\right)_G \\ \bar{\mathbf{F}} &= \hat{\mathbf{F}}\left(\frac{\Delta x}{4}, 0, \frac{\Delta t}{4}\right)_A + \hat{\mathbf{F}}\left(-\frac{\Delta x}{4}, 0, \frac{\Delta t}{4}\right)_C - \hat{\mathbf{F}}\left(-\frac{\Delta x}{4}, 0, \frac{\Delta t}{4}\right)_E - \hat{\mathbf{F}}\left(\frac{\Delta x}{4}, 0, \frac{\Delta t}{4}\right)_G \end{aligned} \quad (16)$$

From Eq. (14) the current space second-order derivatives $(\mathbf{Q}_{xx})_{P'}$ and $(\mathbf{Q}_{yy})_{P'}$ at P' must be known firstly for solving $(\mathbf{Q})_{P'}$. With the estimated value in SE (P') approximated from the last half time step, the current second-order can be expressed as:

$$\begin{aligned} (\mathbf{Q}_{xx})_{P'} &= \frac{(\hat{\mathbf{Q}}_x)_C - (\hat{\mathbf{Q}}_x)_A + (\hat{\mathbf{Q}}_x)_E - (\hat{\mathbf{Q}}_x)_G}{2\Delta x} \\ (\hat{\mathbf{Q}}_x) &= (\mathbf{Q}_x) + \frac{\Delta t}{2} (\mathbf{Q}_{xt}) \end{aligned} \quad (17)$$

$$(\mathbf{Q}_{yy})_{P'} = \frac{(\hat{\mathbf{Q}}_y)_C - (\hat{\mathbf{Q}}_y)_A + (\hat{\mathbf{Q}}_y)_E - (\hat{\mathbf{Q}}_y)_G}{2\Delta y} \quad (18)$$

$$(\hat{\mathbf{Q}}_y) = (\mathbf{Q}_y) + \frac{\Delta t}{2} (\mathbf{Q}_{yt})$$

The cross derivatives $(\mathbf{Q}_{xy})_{P'}$ and $(\mathbf{Q}_{yx})_{P'}$ are:

$$(\mathbf{Q}_{xy})_{P'} = (\mathbf{Q}_{yx})_{P'} = \frac{(\mathbf{Q}_{xy})'_{P'} + (\mathbf{Q}_{yx})'_{P'}}{2} \quad (19)$$

Where

$$(\mathbf{Q}_{xy})'_{P'} = \frac{(\hat{\mathbf{Q}}_x)_C - (\hat{\mathbf{Q}}_x)_A + (\hat{\mathbf{Q}}_x)_E - (\hat{\mathbf{Q}}_x)_G}{2\Delta y} \quad (20)$$

$$(\mathbf{Q}_{yx})'_{P'} = \frac{(\hat{\mathbf{Q}}_y)_C - (\hat{\mathbf{Q}}_y)_A + (\hat{\mathbf{Q}}_y)_E - (\hat{\mathbf{Q}}_y)_G}{2\Delta x}$$

Using the continuous condition at point A' , C' , E' and G' , the left and the right derivatives of $(\mathbf{Q})_{P'}$ in x and y direction can be gained as

$$(\mathbf{Q}_x)_{P'}^- = -\frac{1}{\Delta x} \left[\mathbf{Q} \left(0, \frac{\Delta t}{2} \right)_A + \mathbf{Q} \left(\frac{\Delta t}{2}, 0 \right)_G - \mathbf{Q}_{P'} \right]$$

$$(\mathbf{Q}_x)_{P'}^+ = +\frac{1}{\Delta x} \left[\mathbf{Q} \left(0, 0, \frac{\Delta t}{2} \right)_C + \mathbf{Q} \left(0, 0, \frac{\Delta t}{2} \right)_E - 2(\mathbf{Q})_{P'} \right]$$

$$(\mathbf{Q}_y)_{P'}^- = -\frac{1}{\Delta y} \left[\mathbf{Q} \left(0, 0, \frac{\Delta t}{2} \right)_A + \mathbf{Q} \left(0, 0, \frac{\Delta t}{2} \right)_C - 2(\mathbf{Q})_{P'} \right]$$

$$(\mathbf{Q}_y)_{P'}^+ = +\frac{1}{\Delta y} \left[\mathbf{Q} \left(0, 0, \frac{\Delta t}{2} \right)_E + \mathbf{Q} \left(0, 0, \frac{\Delta t}{2} \right)_G - 2(\mathbf{Q})_{P'} \right] \quad (21)$$

To avoid numerical instability in the case of discontinuity, the derivatives are written in form of weighted average:

$$(\mathbf{Q}_x)_{P'} = W[(\mathbf{Q}_x)_{P'}^-, (\mathbf{Q}_x)_{P'}^+, \alpha] \quad (22)$$

$$(\mathbf{Q}_y)_{P'} = W[(\mathbf{Q}_y)_{P'}^-, (\mathbf{Q}_y)_{P'}^+, \alpha]$$

where α is an adjustable constant and usually equals 1~2 and the weighted equation W is expressed

as

$$W[x_-, x_+, \alpha] = \frac{|x_+|^\alpha x_- + |x_-|^\alpha x_+}{|x_+|^\alpha + |x_-|^\alpha} \quad (23)$$

3.1 Treatments of Stiff Source

The \mathbf{S} is the source term vector of governing equations (1), which are consisted of the production rates of each species. In a reacting flow, the characteristic time of chemistry and flow have a scale gap. The magnitude of stiffness problem can be weighted by the Damkohler number which is defined as the ratio of the maximum characteristic time scale and the minimum's in a

system. For detonation problems:

$$Da = \frac{\tau_{flow}}{\tau_{chem}} \quad (24)$$

where τ_{flow} and τ_{chem} are the characteristic time scale of flow and chemistry reaction, respectively.

Decoupling method was applied to treat the stiff source in this study [15], namely we decoupled the chemistry reaction from governing equations (1), So in one time step, we frozen the reaction and solved the flow field first, then solved the variation of the each species by source

items. And $Da=30$ in this study.

4 Verification of our Improved CE/SE Scheme

In order to verify our improved CE/SE scheme with the second-order accuracy deduced by new structure of CEs and SEs, a detonation propagating in a stoichiometric H_2-O_2 gas was computed. In this case the initial pressure and temperature were 1 atm and 298 K, respectively. Detonation wave was generated by igniting in the left with high initial pressure and temperature 28 atm and 3874 K, respectively. The detailed chemically reacting model was adopted. An mechanism with the eight-species (H_2 , O_2 , H , O , HO , HO_2 , H_2O , H_2O_2) and twenty chemical reactions for hydrogen-oxygen combustion was used [16].

Fig. 2 is the developing process of pressure and temperature simulated. From Fig.2 it can show that deflagration-to-detonation transition (DDT) process completes in very short time and can be ignored. Fig. 3 gives out the numerical results compared with experimental and theoretical results for detonation velocity and CJ pressure. The compared results indicate that they are limited in 3% and the results are very agreement.

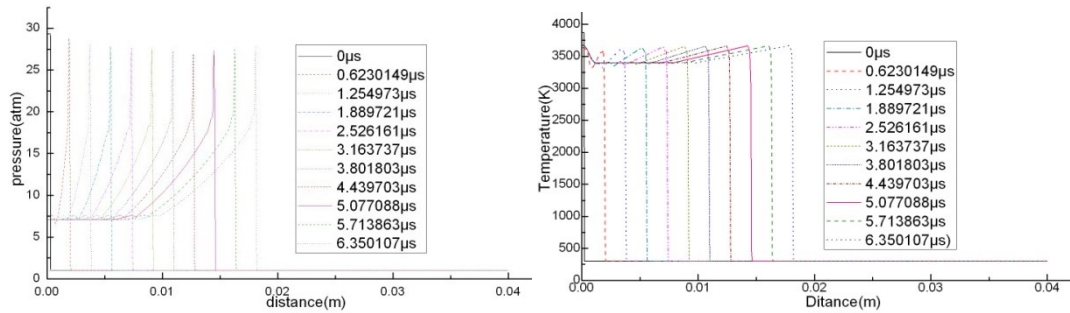


Fig.2 Developing process of pressure and temperature

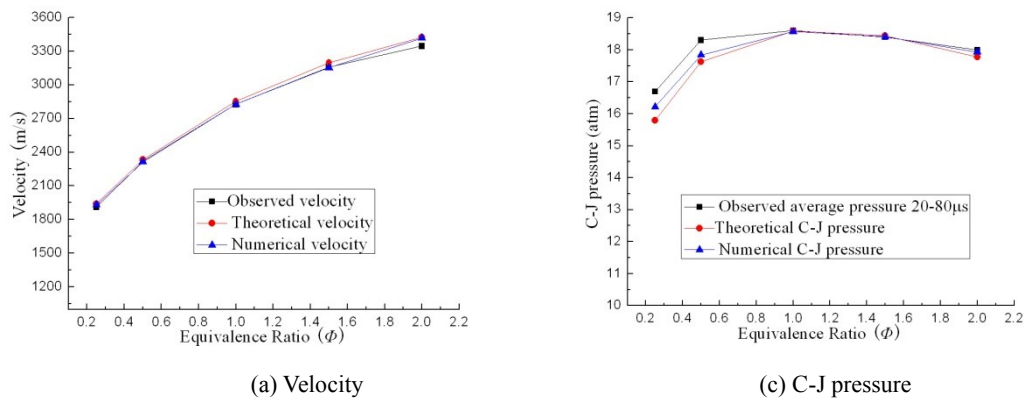


Fig.3. Numerical results compared with experimental and theoretical results

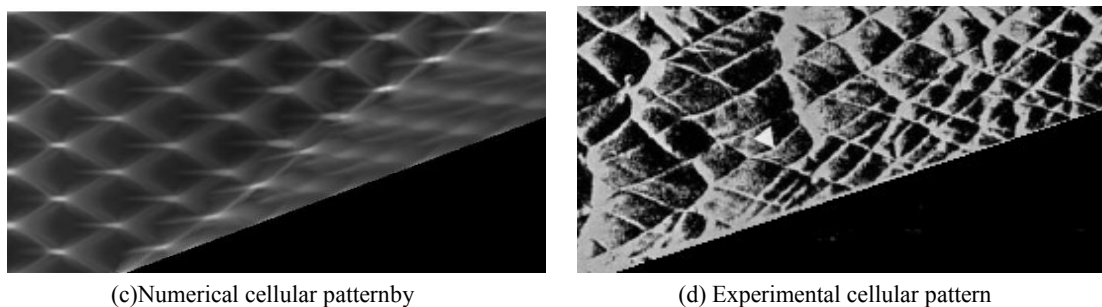


Fig. 4 Cellular pattern of a detonation wave on a 19.3° wedge

Fig.4 shows the cellular patterns produced by the reflection of H_2-O_2 detonation wave over a

19.3° wedge by experiment [17]. The numerical results can agree well with the experiment and numerical results can draw up the basic feature of detonation wave reflection over wedge clearly.

5 Numerical Results

We have completed the numerical simulation of gas-droplet-fueled two-phase detonation by using the Eulerian Two-Fluid Model and Eulerian-Lagrangian Particle-Trace Model and the CE/SE method with the second order accuracy. Their numerical results were compared and analyzed briefly.

5.1 Gas-Droplet-Fueled Detonations with Eulerian-Lagrangian Particle-Trace Model

In the Eulerian-Lagrangian Particle-Trace model it assumed that both droplet phase and gas phase are the continuous and homogeneous medium. The gas phase is governed by Eulerian Eq. (1). However, droplet phase is consisted of particles system and all droplets are traced by using Lagrangian method. Each particle in droplet phase is governed by Lagrangian Eq. (3).

The detonations in liquid $C_{10}H_{22}$ - O_2 /air systems with different fuel droplet radii and equivalence ratios (Φ) have been simulated. Initial pressure and temperature of the mixtures are 1 atm and 298 K, respectively. Detonation wave is generated by igniting in the left with a high initial pressure and temperature as 10 atm and 2980 K, respectively. The other computing parameters are given as below: $\lambda=0.1 \text{ W}\cdot\text{K}^{-1}\cdot\text{m}^{-1}$, $\rho_f=730 \text{ kg/m}^3$, $\mu=2.07\times 10^{-5} \text{ Pa}\cdot\text{s}$, $\mu_f=3.5\times 10^{-4} \text{ Pa}\cdot\text{s}$, $C_v=2.1\times 10^3 \text{ J}\cdot\text{kg}^{-1}\cdot\text{K}^{-1}$, $P_f=0.74$. In the present simulations, the velocity and temperature of the droplets are set to 0 if the radii of the droplets are decreased to 0.

Tang and Nicholls et al. [18] has systematically studied the detonations in a $C_{10}H_{22}$ spray with 200 μm radius droplets in air and oxygen using a vertical shock tube. In order to verify the accuracy of the present model, the detonations in a $C_{10}H_{22}$ spray with 200 μm radius droplets in air and oxygen have been simulated by using Eulerian-Lagrangian Particle-Trace model. The numerical results are compared with theoretical prediction values and experimental data mentioned above. Fig. 6 (a) and (b) show that calculated detonation velocities in our simulation is consistent with the experimental data in trends. Just the calculated results are higher than experimental data.

Meanwhile, we can also find that all theoretical prediction values are agree well with experiment data for mixtures with lean fuel. However, it is worth noting that, for mixtures with rich fuel, all the theoretical prediction values are contrary with experimental value in trends.

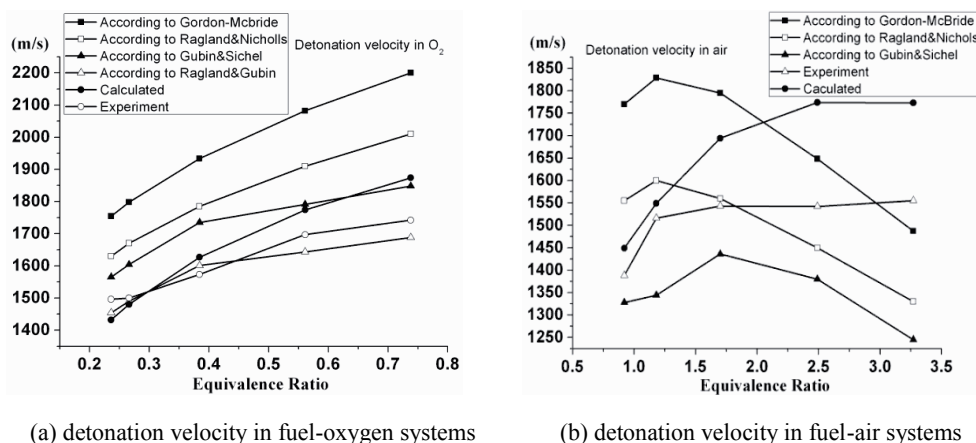


Fig. 6. Comparison of detonation velocity in fuel-oxygen/air systems derived by different methods

Fig. 7 shows the comparison of calculated detonation velocities with C-J theory for all gaseous mixtures. It can be seen that the detonation velocities in O₂ has a similar trend as that in air. Just the detonation velocities in O₂ is higher than that in air.

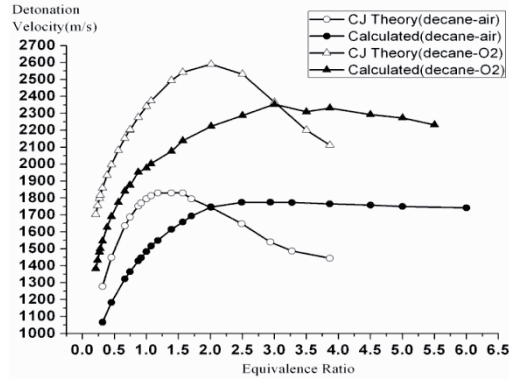


Fig. 7. Comparison of calculated detonation velocity with C-J theory for all gaseous mixtures

5.2 Gas-Droplet-Fueled Detonations with the Eulerian Two-Fluid Model

In order to compare the numerical results obtained with using the Eulerian-Lagrangian Particle-Trace model, we simulated numerically also the Gas-Droplet-Fueled Detonations with the Eulerian Two-Fluid Model.

In the Eulerian Two-Fluid Model it assumed that both droplet phase and gas phase are the continuous and homogeneous medium. The governing equations of gas phase and droplet phase are both Eq. (1): for the gas phase: $\mathbf{Q}=(\rho, \rho u, \rho v, E)^T$, $\mathbf{E}=(\rho u, \rho u^2+p, \rho uv, (E+p)u)^T$, $\mathbf{F}=(\rho v, \rho uv, \rho v^2+p, (E+p)v)^T$, $\mathbf{S}=(I_d, -F_x+u_d I_d, -F_y+v_d I_d, -(u_d F_x+v_d F_y)+((u_d^2+v_d^2)/2+q_r)I_d)^T$, for droplet phase: $\mathbf{Q}=(\rho_d, \rho_d u_d, \rho_d v_d, N)^T$, $\mathbf{E}=(\rho_d u_d, \rho_d u_d^2, \rho_d u_d v_d, Nu)^T$, $\mathbf{F}=(\rho_d v_d, \rho_d u_d v_d, \rho_d v_d^2, N)^T$, $\mathbf{S}=(I_d, -F_x+u_d I_d, -F_y+v_d I_d, 0)^T$, where ρ_d is the density of droplet phase, u_d and v_d are the velocity components of droplet phase, N is the droplet numbers per unit volume, I_d is the density variation by the phase change, F_x and F_y are the forces components acting on droplets, the total energy density $E=p/(\gamma-1)+\rho u^2/2$. The detail of the reduced reaction mechanism can be found in Ref. [19].

The detonations in liquid C₆H₁₄ fuel-air system with different equivalence ratios (Φ) have been simulated. Figure 5 show the detonation velocities of C₆H₁₄ fuel at different equivalence ratios by experiments, C-J theory [20, 21] and simulations, respectively. The numerical results are more accurate than the C-J theoretical values and can agree well with the experimental data. However, the C-J theoretical values are higher than that of the experimental data.

From the results mentioned above we can find that the general trend of the detonations velocities obtained with the Eulerian Two-Fluid Model is consistent with that of the Eulerian-Lagrangian Particle-Trace model.

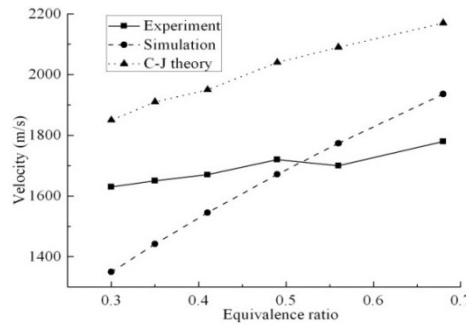


Fig.5 Detonation velocities of C₆H₁₄ fuel at different equivalence ratios

6 Conclusions

The gas-liquid-fueled two-phase detonation is very complex phenomenon, until now we are still the lack of knowledge of the features for gas-liquid-fueled two-phase detonation. In this paper, The Eulerian Two-Fluid Model and Eulerian-Lagrangian Particle-Trace model have been developed and a new framework of the two-dimensional CE/SE method was proposed and deduced. Numerical simulations of detonations in liquid C_6H_{14} fuel-air and $C_{10}H_{22}$ fuel- O_2 /air systems have been achieved. Comparison of numerical simulation with theoretical values and experimental data was completed. Compared results indicate that our simulating results agree well with experimental data in trends. Numerical results obtained by using Eulerian-Lagrangian Particle-Trace model are more accurate than that obtained with Eulerian Two-Fluid Model. However the general trend of the detonations velocities obtained with the Eulerian Two-Fluid Model is consistent with that of the Eulerian-Lagrangian Particle-Trace model.

It is proved that the two models and an improved CE/SE method we proposed above can be successful to simulate gas-liquid-fueled two-phase detonation. Our improved CE/SE scheme has the features of high resolution, simple form and robustness.

References

- [1] Fickett W, Davis W.C, Detonation: Theory & Experiment, Berkeley CA: University of California Press, (1979).
- [2] John H.S. Lee, The Detonation Phenomenon, Cambridge University Press, (2008).
- [3] Charles C Mader, Numerical Modeling of Detonations (LS Series in Basic and Applied Science), University of California Press, (1979).
- [4] Charles C Mader, Recent Advances in Numerical Modeling of Detonations, Propellants, Explosives, Pyrotechnics 11(6) (1986) 163–166.
- [5] Charles C Mader, Numerical Modeling of Explosive & propellants (Third Editions) CRC Press, (2007).
- [6] Dabora E. K., E. K. Weinberger E. K., Present Status of Detonations in Two-Phase Systems, Acta. Astronaut. 1 (3-4) (1974) 361-372.
- [7] Burcat A., Eidelman S., Evolution of a Detonation Wave in a Cloud of Fuel Droplets II. Influence of Fuel Droplets, AIAA J. 18 (10) (1980) 1233-1236.
- [8] Ranger A. A., Nicholls J. A., Aerodynamic Shattering of Liquid Drops, AIAA Journal. 7 (2) (1969) 285-290.
- [9] Eidelman S., Burcat A., Evolution of a Detonation Wave in a Cloud of Fuel Droplet: Part I. Influence of Igniting Explosion, AIAA J. 18 (9) (1980) 1103-1109.
- [10] Westbrook C. K., Dryer F. L., Simplified Reaction Mechanisms for the Oxidation of Hydrocarbon, Combust. Sci. Technol. 27 (1981) 31-43.
- [11] Kiehne T. M., Matthews R. D., et al, An Eight Step Kinetics Mechanism for High Temperature Propane Flames, Combust. Sci. Technol. 54 (1987) 1-23.
- [12] S.C. Chang S.C., The Method of Space-Time Conservation Element and Solution Element-A New Approach for Solving the Navier-Stokes and Euler Equations, J. Comput. Phys. 119 (2) (1995) 295-324.
- [13] Chang S. C., Wang X. Y., Chow C. Y., The Space-Time Conservation Element and Solution

Element Method: A New High-Resolution and Genuinely Multidimensional Paradigm for Solving Conservation Laws, *J. Comput. Phys.* 156 (1) (1999) 89-136.

- [14] Wang G., Zhang D. L., Liu K. X., An Improved CE/SE Scheme and Its Application to Detonation Propagation, *Chin. Phys. Lett.* 24 (2007) 3563-3566.
- [15] Shiro T., Toshi F., Numerical Simulation on the Establishment of Gaseous Detonation, *Progress in Astronautics and Aeronautics*, **94** (1984) 186-200.
- [16] Wang G., Zhang D. L., Liu K. X., Numerical Study on critical Wedge Angle of Cellular Detonation Reflections, *Chin. Phys. Lett.* 27 (2010) 024701.
- [17] C. M. Guo, D. L. Zhang, W. Xie, The Mach Reflection of a Detonation Based on Soot Track Measurements, *Combustion and Flame*, **127** (2001) 2051-2058.
- [18] Tang M. J., Nicholls J. A., Sichel M., Lin Z. C., The Direct Initiation of Detonation in Decane-Air and Decane-Oxygen Sprays, Gas dynamics laboratories, report No. UM-018404-1, October 1983.
- [19] Wang T.S., Thermophysics characterization of kerosene combustion, AIAA 2000-2511, 2000.
- [20] E.K. Dabora E.K., Ragland K.W., Nicholls J.A., A study of heterogeneous detonations, *Astronautica Acta* 12 (1966) 9-16.
- [21] Roy G.D., Frolov S.M., Borisov A.A., Netzer D.W., Pulse detonation propulsion: challenges, current status, and future perspective, *Progress in Energy and Combustion Science* 30 (2004) 545-672.